Angiotensin II signaling via protein kinase C phosphorylates Kelch-like 3, preventing WNK4 degradation

Shigeru Shibata[a,b,c,d,1,2], Juan Pablo Arroyo[a,d,1], María Castañeda-Bueno[a,d], Jeremy Puthumana[a,d], Junhui Zhang[a,d], Shunya Uchida[b], Kathryn L. Stone[e], TuKiet T. Lam[e], and Richard P. Lifton[a,d,2]

Departments of [a]Genetics and [e]Molecular Biophysics and Biochemistry and [d]Howard Hughes Medical Institute, Yale University School of Medicine, New Haven, CT 06510; [b]Division of Nephrology, Department of Internal Medicine, Teikyo University School of Medicine, Tokyo 173-8605, Japan; and [c]Department of Clinical Epigenetics, Research Center for Advanced Science and Technology, University of Tokyo, Tokyo 153-0041, Japan

Contributed by Richard P. Lifton, September 23, 2014 (sent for review March 3, 2014; reviewed by Thomas M. Coffman and David Pearce)

Hypertension contributes to the global burden of cardiovascular disease. Increased dietary K^+ reduces blood pressure; however, the mechanism has been obscure. Human genetic studies have suggested that the mechanism is an obligatory inverse relationship between renal salt reabsorption and K^+ secretion. Mutations in the kinases with-no-lysine 4 (WNK4) or WNK1, or in either Cullin 3 (CUL3) or Kelch-like 3 (KLHL3)—components of an E3 ubiquitin ligase complex that targets WNKs for degradation—cause constitutively increased renal salt reabsorption and impaired K^+ secretion, resulting in hypertension and hyperkalemia. The normal mechanisms that regulate the activity of this ubiquitin ligase and levels of WNKs have been unknown. We posited that missense mutations in KLHL3 that impair binding of WNK4 might represent a phenocopy of the normal physiologic response to volume depletion in which salt reabsorption is maximized. We show that KLHL3 is phosphorylated at serine 433 in the Kelch domain (a site frequently mutated in hypertension with hyperkalemia) by protein kinase C in cultured cells and that this phosphorylation prevents WNK4 binding and degradation. This phosphorylation can be induced by angiotensin II (AII) signaling. Consistent with these in vitro observations, AII administration to mice, even in the absence of volume depletion, induces renal $KLHL3^{S433}$ phosphorylation and increased levels of both WNK4 and the NaCl cotransporter. Thus, AII, which is selectively induced in volume depletion, provides the signal that prevents CUL3/KLHL3-mediated degradation of WNK4, directing the kidney to maximize renal salt reabsorption while inhibiting K^+ secretion in the setting of volume depletion.

renin–angiotensin–aldosterone system | distal tubule | hypertension | posttranslational modification | PHAII

Hypertension affects 1 billion people worldwide and is a major risk factor for death from stroke, myocardial infarction, and congestive heart failure. The study of Mendelian forms of hypertension has demonstrated the key role of increased renal salt reabsorption in disease pathogenesis (1–4). Observational and intervention trials (5, 6) also indicate that increased dietary K^+ lowers blood pressure; however, the mechanism of this effect has been unclear.

Pseudohypoaldosteronism type II (PHAII; Online Mendelian Inheritance in Man no. 145260), featuring hypertension and hyperkalemia, has revealed a previously unrecognized mechanism that regulates the balance between renal salt reabsorption and K^+ secretion in response to aldosterone (7). Aldosterone is produced by the adrenal glomerulosa in volume depletion, in response to angiotensin II (AII), and in hyperkalemia via membrane depolarization (8). In volume depletion, aldosterone maximizes renal salt reabsorption, whereas in hyperkalemia, aldosterone promotes maximal renal K^+ secretion. Volume depletion increases both the NaCl cotransporter (NCC) (9) and electrogenic Na^+ reabsorption via the epithelial Na^+ channel (ENaC) (10). The lumen-negative potential produced by ENaC activity provides the electrical driving force for paracellular Cl^- reabsorption (11). In hyperkalemia, the lumen-negative potential promotes K^+ secretion via the K^+ channel Kir1.1 (renal outer medullary K^+ channel ROMK), reducing plasma K^+ level (12, 13). Additionally, recent studies have implicated aldosterone signaling in intercalated cell transcellular Cl^- flux (14). In these cells, hyperkalemia induces phosphorylation of the mineralocorticoid receptor (MR) ligand-binding domain, making it incapable of ligand binding and activation. AII signaling induces dephosphorylation, and activation of the MR by aldosterone then induces transcellular Cl^- flux, which is required for defense of intravascular volume (14, 15). Because electrogenic Cl^- reabsorption and K^+ secretion both dissipate the lumen-negative potential produced by ENaC, maximal Cl^- reabsorption inhibits K^+ secretion and vice versa.

Patients with PHAII have constitutive reabsorption of NaCl with concomitant inhibition of K^+ secretion, resulting in hypertension and hyperkalemia, despite normal levels of aldosterone (7). Dominant mutations in the serine–threonine kinases with-no-lysine 4 (WNK4) or WNK1, or in CUL3 or KLHL3, elements of a ubiquitin ligase complex, cause this disease (2, 4). WNK4 modulates the activities of NCC, ENaC, Kir1.1, and MR (14,

Significance

Aldosterone produces distinct adaptive responses in volume depletion and hyperkalemia. Mutations in with-no-lysine (WNK) kinases or ubiquitin ligases containing Cullin 3 (CUL3) and Kelch-like 3 (KLHL3) cause a Mendelian disease featuring hypertension and hyperkalemia due to constitutive renal salt reabsorption and inhibited K^+ secretion. WNKs modulate activities of aldosterone-regulated electrolyte flux pathways, and WNK levels are regulated by CUL3/KLHL3; disease-causing mutations prevent WNK degradation. This manuscript shows that angiotensin II (AII), a hormone produced only in volume depletion, induces PKC-mediated phosphorylation of KLHL3, preventing WNK degradation and phenocopying KLHL3 mutations. These findings provide a mechanism by which AII signaling alters WNK4, promoting increased renal salt reabsorption and reduced K^+ secretion.

Author contributions: S.S., J.P.A., and R.P.L. designed research; S.S., J.P.A., M.C.-B., J.P., and J.Z. performed research; S.U. contributed new reagents/analytic tools; S.S., J.P.A., K.L.S., T.T.L., and R.P.L. analyzed data; and S.S., J.P.A., and R.P.L. wrote the paper.

Reviewers: T.M.C., Duke University and Durham VA Medical Centers; and D.P., University of California, San Francisco.

The authors declare no conflict of interest.

Freely available online through the PNAS open access option.

[1]S.S. and J.P.A. contributed equally to this work.

[2]To whom correspondence may be addressed. Email: richard.lifton@yale.edu or shigeru.shibata@med.teikyo-u.ac.jp.

This article contains supporting information online at www.pnas.org/lookup/suppl/doi:10.1073/pnas.1418342111/-/DCSupplemental.

16–21), and WNK4 function can be modulated by phosphorylation (21). CUL3/KLHL3 has been shown to target WNK4 and WNK1 for ubiquitination and degradation, and disease-causing mutations impair this binding and degradation (22–24). In particular, dominant mutations in the Kelch domain of KLHL3 prevent binding to WNKs; reciprocally, disease-causing point mutations in WNK4 also prevent WNK4–KLHL3 binding.

These findings suggest that regulation of WNK degradation by CUL3/KLHL3 is highly regulated and that disease-causing mutations might phenocopy a state in which WNKs are normally turned off, producing constitutive salt reabsorption and inhibited K^+ secretion. We now demonstrate that this inference is correct and implicate AII signaling in this process.

Results

Identification of Phosphorylation Sites in KLHL3. FLAG-epitope–tagged human KLHL3 (23) was expressed in COS-7 cells and purified by immunoprecipitation (IP) and SDS/PAGE. After TiO_2 affinity chromatography, phosphopeptides and specific phosphorylation sites were identified by liquid chromatography (LC) and tandem mass spectrometry (MS/MS) (14). In three independent mapping experiments, we reproducibly observed four phosphorylation sites: one at the N terminus, two between the BACK (BTB and C-terminal Kelch) and Kelch domains, and one in the Kelch domain (Fig. 1*A* and Table S1).

Phosphorylation at S433 in the Kelch domain (Fig. 1*B*; average Mascot ion score of 78) was of particular interest. This site lies in a "d–a" loop between successive blades of the Kelch propeller; these loops are involved in substrate binding (25). S433 and flanking sequences are completely conserved in orthologs through zebrafish (Fig. 1*C*). Interestingly, S433 is recurrently mutated in autosomal dominant PHAII (4, 26). Mutation of S433 abrogates WNK4 binding and degradation, increasing WNK4 levels (22, 23). This observation suggested that S433 phosphorylation might modulate KLHL3 binding and degradation of WNK4.

KLHL3 Phosphorylation at S433 Prevents WNK4 Binding and Degradation. Plasmids encoding wild-type KLHL3 ($KLHL3^{WT}$) or mutant KLHL3 with phosphomimetic glutamate substitution ($KLHL3^{S433E}$), both with N-terminal FLAG-epitope tags, were expressed in COS-7 cells and purified by IP with anti-FLAG. In parallel, WNK4–HA was purified by IP with anti-HA. FLAG–$KLHL3^{WT}$ or –$KLHL3^{S433E}$ was incubated with WNK4–HA, and IP was performed with anti-FLAG, followed by Western blotting with anti-HA to detect WNK4. These experiments were performed in vitro to ensure that equal amounts of protein were input into all experiments, eliminating the confounding effect of KLHL3 causing WNK4 degradation in vivo (23). Whereas $KLHL3^{WT}$ robustly bound WNK4, $KLHL3^{S433E}$ showed almost no binding (Fig. 2*A*).

We consequently expected that phosphorylation of KLHL3 at S433 would reduce degradation and increase WNK4 levels in cells. We quantitated WNK4 levels when expressed with either $KLHL3^{WT}$ or $KLHL3^{S433E}$ (23). As reported (23), $KLHL3^{WT}$ reduced WNK4 levels by 57% ($P = 0.002$; Fig. 2*B*). In contrast, $KLHL3^{S433E}$ produced no significant change in WNK4 levels (10% increase, $P = 0.34$; Fig. 2*B*).

AII Signaling Increases Phosphorylation of $KLHL3^{S433}$. Multiple lines of evidence suggest that WNK4 lies downstream of AII signaling (14, 27, 28), suggesting that AII regulates WNK4 levels via phosphorylation of $KLHL3^{S433}$ (23, 29). Angiotensin type 1 receptor (AT1R) activation by AII induces release of the G protein alpha subunit, G_q, which leads to activation of protein kinase C (PKC) (30). The basic residues flanking S433 in KLHL3 ($RRSS^{433}$) constitute a canonical PKC motif and are predicted to be a PKC phosphorylation site by NetPhorest (31).

FLAG–KLHL3 was purified from COS-7 and subjected to Western blotting by using a monoclonal antibody that recognizes $RRXS^P$ (α-$RRXS^P$). Whereas $KLHL3^{WT}$ was strongly stained, $KLHL3^{S433N}$ or $KLHL3^{S433A}$ were not (Fig. 3*A*). These results confirm the presence of $KLHL3^{S433\text{-}P}$ in COS-7 and the specificity of this antibody for KLHL3 phosphorylated at S433.

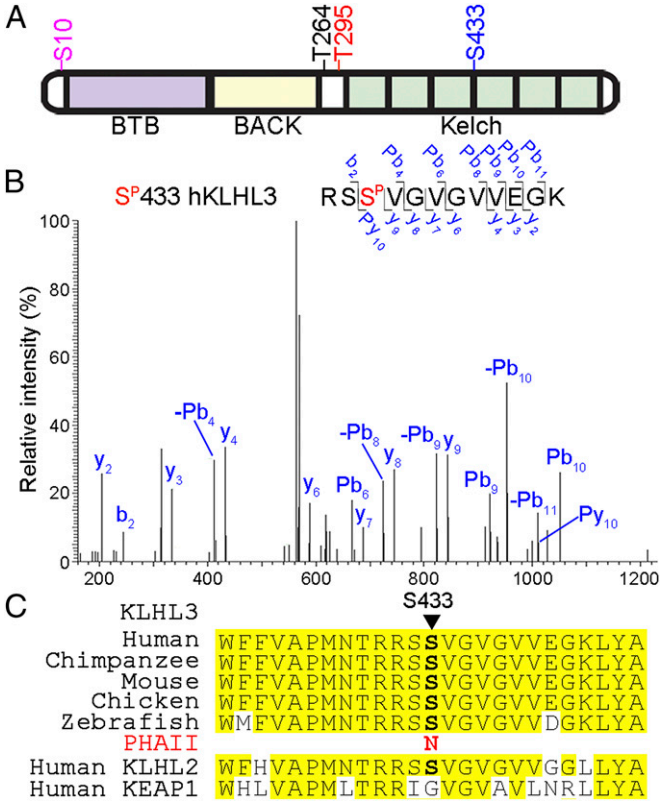

Fig. 1. Phosphorylation sites in human KLHL3. (*A*) Sites phosphorylated in KLHL3 in COS-7 cells are shown. Sites in motifs suggesting phosphorylation by proline-directed kinase (red), protein ATM kinase (magenta), protein kinase C (blue), or no known kinase (black) are indicated. See also Table S1, which shows the list of phosphopeptides identified by MS/MS. (*B*) MS/MS spectrum of phosphopeptide containing S433-P is shown. The phosphorylated precursor ion, which has a mass of 627.32^{2+}, was selected and produced the fragment ion spectrum shown. Specific y and b ions allowed assignment of phosphorylation at S433. Fragment ions with neutral loss of phosphate are indicated (–Pb_4, etc). (*C*) Conservation of S433 among KLHL3 orthologs. This segment is highly conserved among orthologs, and the paralog KLHL2. S433 has been found mutated to asparagine (N) in independent kindreds with PHAII (red). At the bottom are the sequences of human KLHL2 and KEAP1.

We next examined whether AII signaling increases $KLHL3^{S433\text{-}P}$ in cell lines. HEK cells have the machinery for AII signaling when AT1R is expressed (32). HEK cells show low levels of phosphorylation of $KLHL3^{S433}$, which is eliminated by S433N substitution (Fig. 3*B*). AT1R and FLAG–KLHL3 were expressed in HEK cells and incubated in serum-free medium with or without 250 nM AII [similar to AII levels previously used to induce signaling (32)]. KLHL3 was immunoprecipitated from lysates of these cells, and Western blotting was performed with α-$RRXS^P$. AII significantly increased $KLHL3^{S433\text{-}P}$ at both 5 and 30 min (1.8-fold; $P = 0.0001$, three independent experiments; and 2.4-fold, $P = 0.008$, four independent experiments, respectively; Fig. 3*B*).

PKCα and PKC-β Directly Phosphorylate KLHL3 at S433. Because AII activates PKC, we expected that inhibition of PKC would prevent AII-induced increases in $KLHL3^{S433\text{-}P}$. Bisindolylmaleimide I, a specific PKC inhibitor, but not the PKA inhibitor H89, significantly reduced AII-induced increases in $KLHL3^{S433\text{-}P}$ (Fig. S1).

Among PKC isozymes, PKC-α, PKC-β, and PKC-ε are downstream of AII signaling in renal epithelia, vasculature, and adrenal grand (33–35). All three isozymes are expressed in COS-7 and

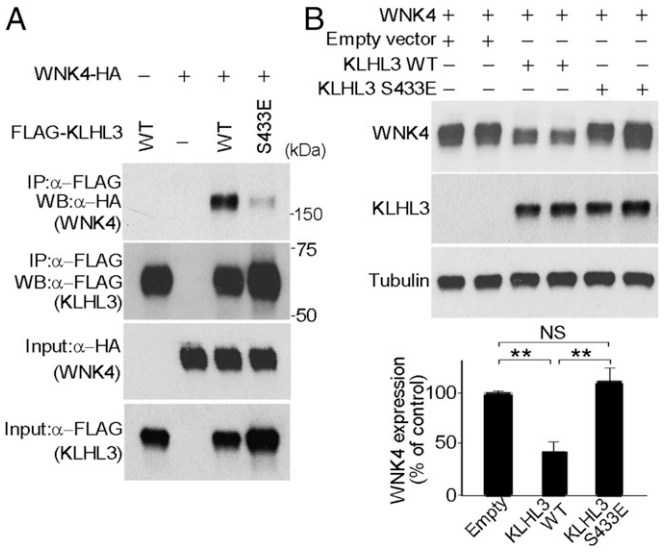

Fig. 2. Phosphomimetic substitution KLHL3^{S433E} prevents binding and degradation of WNK4. (*A*) FLAG–KLHL3^{WT} and –KLHL3^{S433E} were purified by IP from COS-7 cells and incubated with purified WNK4^{WT}–HA followed by FLAG–IP and Western blotting (WB). KLHL3^{S433E} virtually eliminates binding of WNK4. (*B*) Western blots of cell lysates coexpressing indicated proteins are shown. Transfection of KLHL3^{WT} markedly reduces WNK4 level; in contrast, KLHL3^{S433E} has no significant effect on WNK4 level. An empty vector was used as a control to equalize the total amount of DNA in transfections lacking KLHL3. Bar graphs show the results of quantitation ($n = 5$). Data are expressed as means ± SEM. $^{**}P < 0.01$. NS, not significant.

HEK cells (36, 37). We incubated purified FLAG–KLHL3 with ATP and 0.3 units of PKC-α, PKC-βI, or PKC-ε in vitro. PKC-α and PKC-βI both markedly increased KLHL3^{S433-P} (15.5- and 10.1-fold, respectively), whereas PKC-ε had a much smaller effect (Fig. 3*C*; PKCε phosphorylated control substrate peptide; Fig. S2). S433N substitution abolished the signal (Fig. 3*D*).

AII Signaling Prevents KLHL3-Mediated Reduction of WNK4 in HEK Cells. Induction of KLHL3^{S433-P} by AII suggested that AII signaling should prevent KLHL3-mediated degradation of WNK4. We coexpressed WNK4, KLHL3, and AT1R in HEK cells and incubated cells with AII for 6 h after 12 h in serum-free medium. Cells were then lysed, and WNK4 levels were quantitated. Expression of KLHL3 reduced WNK4 levels by 80%, a larger effect than in COS-7 cells, owing to lower basal phosphorylation of S433. Although AII did not alter WNK4 levels in the absence of KLHL3, in its presence, AII produced dose-dependent increases in WNK4 (threefold increase at 250 nM AII; $P = 0.0001$; Fig. 4*A*). This effect was nearly completely blocked by preincubation with the AT1R blocker (ARB) losartan (Fig. 4*B*).

Finally, knockdown of *PRKCA* by RNA interference (siRNA) markedly reduced PKC-α protein levels and prevented AII-induced increases in WNK4 levels (Fig. 4 *C* and *D*).

AII Infusion Increases KLHL3^{S433-P} and WNK4 Levels in Vivo. From these effects in cell culture, AII signaling, even without volume depletion, should increase renal WNK4 levels. C57/B6 mice on high-NaCl diet received continuous infusion of AII (1 μg/kg per min, s.c. for 48 h), and WNK4 levels were measured. AII significantly increased WNK4 levels in mouse kidney (1.5-fold, $P = 0.0012$; seven independent animals studied; Fig. 5). Total KLHL3 levels were unaltered.

To determine whether AII's effect was mediated by increased KLHL3^{S433-P}, we produced a polyclonal antibody to KLHL3^{S433-P}. This antibody recognized KLHL3 peptide phosphorylated at S433, but not unphosphorylated peptide (Fig. 6*A*). Moreover, Western blotting using this antibody with lysates from COS-7 cells expressing KLHL3^{WT} identified KLHL3; this signal was absent in cells expressing no KLHL3 or KLHL3 in which S433 is mutated to alanine (Fig. 6*B*). Specificity was further demonstrated by Western blotting of immunoprecipitated FLAG-KLHL3^{WT} and –KLHL3^{S433A} (Fig. 6*C*).

Previous studies have demonstrated that both WNK4 and KLHL3 are present in the thick ascending limb of Henle (TAL), distal convoluted tubule (DCT), connecting tubule (CNT), and collecting duct (CD) (2, 4, 26, 38). Levels of KLHL3^{S433-P} in nephrons of mice on a high-salt diet with and without AII infusion (five mice in each group) was compared by immunofluorescence microscopy. The results showed very low levels of KLHL3^{S433-P} without but a marked increase with AII infusion. Costaining revealed that KLHL3^{S433-P} was increased in nephron segments that also stain for calbindin D-28-K, a marker for DCT (Fig. 6*D*), the Na^+-K^+-$2Cl^-$ cotransporter (NKCC2), a marker of TAL, and aquaporin 2, a marker of CNT and CD (Fig. 6*E* and Fig. S3). KLHL3^{S433-P} signals were eliminated by competition with immunizing phosphopeptide (Fig. S3*B*). KLHL3^{S433-P} was present at the apical membrane and cell–cell junctions (Fig. S3*C*), resembling the subcellular distribution of WNK4 (2, 14, 23). As expected, AII infusion significantly increased membrane NCC levels (2.4-fold, $P = 0.03$; Fig. S3 *D* and *E*).

Discussion

Classically, stimulation of renal salt transport in volume depletion is attributed to increased aldosterone signaling, whereas

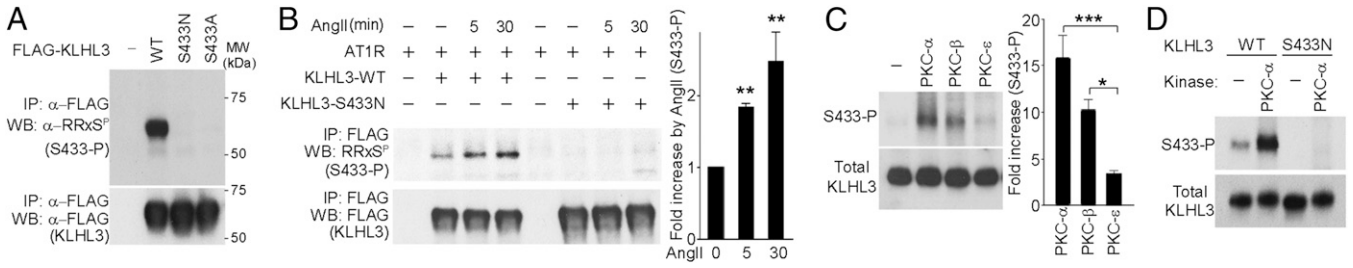

Fig. 3. AII signaling and PKC increase KLHL3^{S433-P}. (*A*) Wild-type FLAG–KLHL3 and –KLHL3 with S433N or S433A substitution were purified by IP from COS-7 and subjected to Western blotting with α-RRxS^P and α-FLAG. Although a robust signal is detected by α-RRxS^P with KLHL3^{WT}, no signal is detected with KLHL3^{S433N} or KLHL3^{S433A}, indicating that the antibody is recognizing phosphorylation at S433. (*B*) HEK cells expressing AT1R and either FLAG–KLHL3^{WT} or –KLHL3^{S433N} were incubated with 250 nM AII for 5 or 30 min. Cell lysates were immunoprecipitated with anti-FLAG, followed by Western blotting with α-RRxS^P. Bar graphs show quantitation of the results ($n = 3$ or 4), demonstrating that AII induces increased phosphorylation at S433. (*C*) FLAG-tagged KLHL3 was expressed in COS-7 cells, purified by IP, and incubated with indicated PKC isoforms in the presence of ATP (*Materials and Methods*). KLHL3^{S433-P} was detected by Western blotting with α-RRxS^P, and total KLHL3 was detected by FLAG antibody. KLHL3^{S433-P} signal is highly induced by PKC-α and, to a lesser extent, by PKC-β. PKC-ε has small effects on KLHL3^{S433-P} levels. Bar graphs show quantitation of the results of four to six independent experiments in each condition. (*D*) Phosphorylation at S433 is abolished by S433N substitution without altering total KLHL3 levels. Data are expressed as means ± SEM. $^{*}P < 0.05$; $^{**}P < 0.01$; $^{***}P < 0.001$.

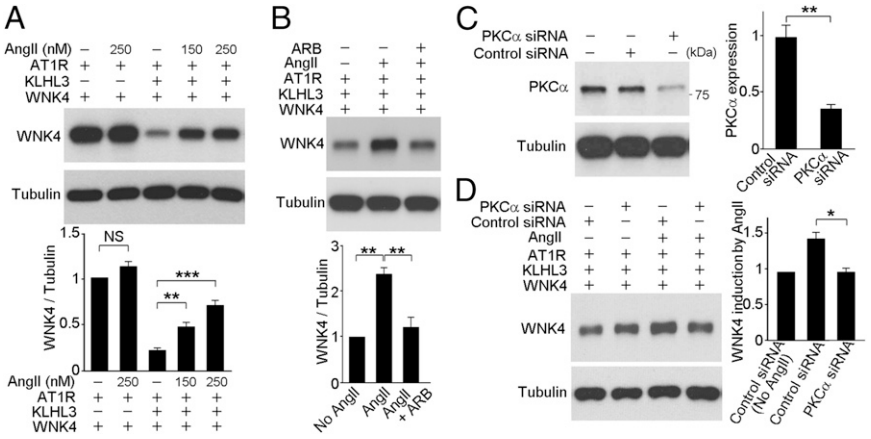

Fig. 4. AII signaling prevents KLHL3-mediated degradation of WNK4. (*A*) AT1R and WNK4 were expressed in HEK cells with or without KLHL3 and with or without incubation with AII (150 or 250 nM) for 6 h. Levels of WNK4 were quantitated by Western blotting with α-HA. Bar graph shows the results of quantitation ($n = 4$ each group). Expression of KLHL3 in the absence of AII reduces WNK4 level by 80%. Whereas AII has no effect on WNK4 in the absence of KLHL3, AII reverses KLHL3-induced reduction in WNK4 levels in a dose-dependent manner. (*B*) HEK cells expressing AT1R, KLHL3, and WNK4 were incubated with 250 nM AII with or without the pharmacologic AT1R blocker (ARB) losartan for 6 h. The ability of AII signaling to increase WNK4 level is prevented by coincubation with losartan. Bar graphs show the results of quantitation ($n = 4$). (*C*) Quantitative analysis of PKC-α protein expression in HEK cells cotransfected with indicated siRNAs and FLAG–KLHL3 ($n = 3$). Addition of siRNA to *PRKCA* reduces PKC-α level by 70%. (*D*) HEK cells expressing AT1R, KLHL3, and WNK4 plus indicated siRNAs were incubated with or without AII for 6 h. WNK4 levels in the cell lysates were quantitated ($n = 4$). Addition of siRNA to *PRKCA* prevents AII-induced increase in WNK4. Data are expressed as means ± SEM. $*P < 0.05$; $**P < 0.01$; $***P < 0.001$. NS, not significant.

the major physiologic effects of AII signaling are ascribed to induction of aldosterone biosynthesis and arterial vasoconstriction (8, 39). It is increasingly recognized, however, that AII also directly affects renal epithelia. AT1R is present throughout the nephron (40), and signaling increases activities of the sodium hydrogen exchanger 3 in the proximal tubule, NKCC2 in the TAL, NCC of the DCT, and ENaC in the CNT and CD (41–44). AII also regulates phosphorylation and activity of MR in renal intercalated cells, allowing induction of a transcellular Cl^- reabsorption pathway (14). In addition, AII signaling inhibits ROMK activity, inhibiting renal K^+ secretion (45).

In parallel, mutations in WNK1, WNK4, KLHL3, and CUL3 led to the recognition that WNKs regulate the activities of diverse mediators of salt reabsorption and K^+ secretion. Mutations in WNK4 that cause hypertension and hyperkalemia promote activity of mediators of salt reabsorption while inhibiting mediators of K^+ secretion (14, 16–21), and AII signaling in intercalated cells requires WNK4 (14).

The present findings link these observations, demonstrating that AII signaling phenocopies the effects of mutation in KLHL3 that cause increased salt reabsorption and inhibition of K^+ secretion. AII signaling activates PKC, which phosphorylates S433 in KLHL3, preventing WNK4 binding and resulting in increased WNK4 levels. S433 lies in the Kelch domain of KLHL3 and is recurrently mutated in patients with PHAII (4, 26). In vivo experiments showed that AII infusion caused increased levels of both $KLHL3^{S433\text{-}P}$ and WNK4 and the downstream target NCC. These findings provide evidence that AII provides the signal that allows the kidney to discriminate between volume depletion and hyperkalemia (Fig. S4).

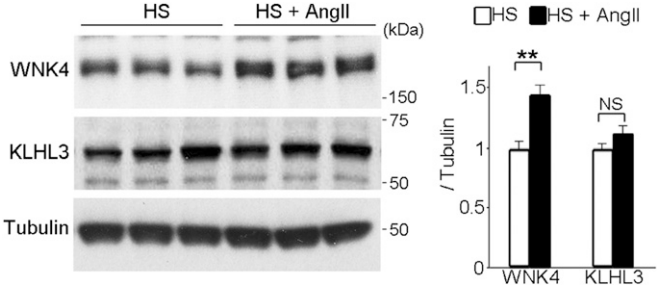

Fig. 5. AII increases WNK4 levels in vivo. C57/B6 mice eating a high-salt (HS) diet received continuous infusion of AII (1 μg/kg per min, s.c.) for 48 h, after which renal levels of WNK4 and KLHL3 were measured by Western blotting. Bar graphs show the results of quantitation ($n = 7$). The results demonstrate a 45% increase in levels of WNK4 without change in KLHL3 level. Data are expressed as means ± SEM. $**P < 0.01$. NS, not significant.

The significance of these AII effects is supported by the effects of point mutations in KLHL3 that alter S433; these single mutations result in hypertension and hyperkalemia that can be corrected by inhibitors of NCC (4, 26). Thus, although AII signaling might have other downstream effects in renal epithelia, the effects on KLHL3 alone are sufficient for marked clinical impact. The effects of AII signaling in renal epithelia are further supported by the results of renal transplantation between wild-type mice and mice deficient for *Agtr1a*, which showed that the absence of renal AT1R reduces blood pressure (46).

These findings are also consistent with studies demonstrating that phosphorylation can either negatively (47) or positively (48) regulate the activity of E3 ubiquitin ligases. KLHL2, which can also bind WNK4 (49), may be regulated by the same mechanism, because the segment spanning S433 in KLHL3 is virtually identical in KLHL2 (Fig. 1*C*). KLHL2 is highly expressed in the brain, with lower expression in other tissues (50). Because virtually all PHAII kindreds are accounted for by mutations in *WNK1, WNK4, KLHL3*, and *CUL3* (4), and no mutations in *KLHL2* have been found, we think it is unlikely that this gene plays a role like *KLHL3* in regulation of renal WNK4/WNK1; however, a role in the regulation of WNK4 in neurons and/or glia is an interesting possibility for future exploration (51).

Among other phosphorylation sites identified in KLHL3 in this study, S10 occurs in an SQ motif, which is recognized by ATM (ataxia telangiectasia mutated kinase), which regulates several E3 ubiquitin ligases (52–55). Given that these other sites in KLHL3 are located outside the Kelch domain, their physiological significance is unclear. Determining the functional consequences of phosphorylation at these other KLHL3 sites will require further investigation.

Besides its effect on WNK4 levels, it seems likely that AII signaling has additional effects on WNK1 and/or WNK4 function. WNK4 expression alone inhibits NCC (17, 18, 27, 56) and does not result in stimulation of the Ste20-related proline alanine rich kinase–NCC cascade and Na^+ reabsorption (27). AII might also induce phosphorylation of WNKs, thereby modulating the activity of electrolyte flux pathways. Further studies will be required to explore this possibility.

$KLHL3^{S433}$ might also be phosphorylated by other kinases. In addition, this site is predicted by NetPhorest to be a substrate of PKA, the cAMP-activated kinase. Given evidence that several Gs-coupled G protein-coupled receptors [including the vasopressin V2 receptor (57) and β-adrenergic receptors (58)] regulate NKCC2 via PKA, it will be of interest to examine whether phosphorylation of $KLHL3^{S433}$ regulates transport activity in TAL.

MEDICAL SCIENCES

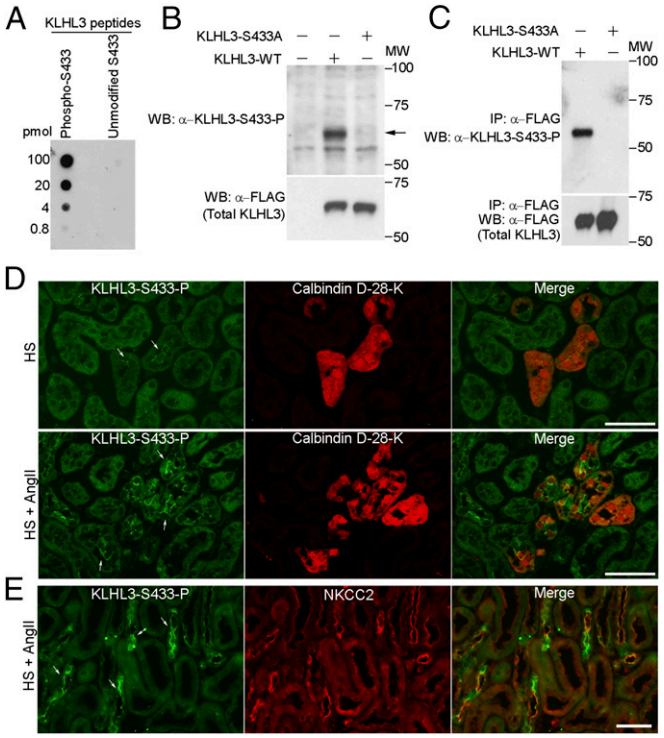

Fig. 6. AII increases KLHL3$^{S433\text{-}P}$ in vivo in kidney. (*A*) Phosphorylated and nonphosphorylated KLHL3 peptides were spotted on a nitrocellulose membrane and incubated with α-KLHL3$^{S433\text{-}P}$, followed by staining with peroxidase-conjugated donkey anti-rabbit antibody. The results demonstrate the specificity of the antibody for the phosphopeptide. (*B*) Total cell lysates from COS-7 expressing no KLHL3, FLAG–KLHL3^{WT}, and –KLHL3^{S433A} were analyzed by Western blotting (WB) using α-KLHL3$^{S433\text{-}P}$ (*Upper*) and anti-FLAG (*Lower*) antibodies. Serine to alanine substitution at position 433 in KLHL3 eliminates the signal at the expected molecular weight (arrow). (*C*) FLAG–KLHL3^{WT} and –KLHL3^{S433A} were purified by FLAG-IP from COS-7 cells and were analyzed by WB using the indicated antibodies. α-KLHL3$^{S433\text{-}P}$ recognizes purified KLHL3^{WT}, but not nonphosphorylatable KLHL3^{S433A}, further confirming specificity of the antibody. (*D*) C57/B6 mice eating a high-salt (HS) diet either did or did not receive continuous infusion of AII. After 48 h, kidneys were sectioned and immunostained with α-KLHL3$^{S433\text{-}P}$ and α-Calbindin D-28-K (a DCT marker). Arrows indicate staining for KLHL3$^{S433\text{-}P}$. The KLHL3$^{S433\text{-}P}$ level is very low in mice on a high-salt diet without AII (*Left*). Signal intensity is markedly increased in mice on high-salt diet that received AII infusion ($n = 5$). (Scale bars, 50 μm.) (*E*) Kidneys from mice on high-salt diet plus AII infusion were sectioned and immunostained with α-KLHL3$^{S433\text{-}P}$ and α-NKCC2, a marker of TAL. Arrows indicate KLHL3$^{S433\text{-}P}$ staining. (Scale bar, 50 μm.) Results demonstrate KLHL3$^{S433\text{-}P}$ in TAL. See also Fig. S3.

Similarly, this phosphorylation may play a role in regulation of transport in principal and intercalated cells (14). Multiple hormonal signaling pathways may converge on this site in regulating electrolyte flux in renal epithelia.

Materials and Methods

Plasmids. The cDNAs used in this study included FLAG–KLHL3 (23), WNK4–HA (23), and AT1R (27). The S433E, S433N, and S433A mutations were introduced into KLHL3 by using the QuikChange site-directed mutagenesis system (Stratagene). siRNAs targeting *PRKCA* (s11092) and negative control (negative control no. 2) were purchased from Life Technologies. Knockdown efficiency and specificity of siRNAs used in this study have been validated by the vendor, and efficiency of knockdown was reproduced in the present study.

LC-MS/MS. Mass spectrometry was performed at the Yale W. M. Keck Foundation Biotechnology Resource Laboratory as described (14). FLAG-tagged KLHL3 expressed in COS-7 cells was immunoprecipitated by using anti-FLAG antibodies followed by SDS/PAGE. The resulting protein was digested in the gel with trypsin, and phosphopeptides were enriched by using TiO_2 affinity. They were analyzed by LC-MS/MS using an LTQ Orbitrap Elite equipped with a WatersNanoACQUITY ultra-performance LC system. All MS/MS spectra were searched by using the Mascot search engine. Phosphorylation site scoring was carried out with MASCOT delta and phosphoRS algorithms. Phosphopeptide identities were confirmed by manual inspection.

Transient Transfection and IP. Transient transfection of plasmid DNA was carried out by using cationic liposome (9 μg per plate for a 10-cm plate or 1 μg per well for a six-well plate; Lipofectamine 2000; Life Technologies). In cotransfection of different DNAs, each DNA was mixed at a ratio of 1:1, except triple transfection of WNK4–HA, AT1R, and FLAG–KLHL3 (in these experiments described in Fig. 4, DNAs were mixed at a ratio of 1 [WNK4]:1 [AT1R]:0.1 [KLHL3]). Cotransfection of plasmid DNA and siRNA was carried out by using nonliposomal polymer (TransIT-X2; Mirus Bio). DNAs (2.5 μg per well), siRNA (5 μL of 20 μM concentration), and TransIT-X2 reagent (15 μL) were mixed in Opti-MEM (final volume: 250 μL). After 30 min of incubation, the mixture was added to 2.5 mL of the cell culture medium. After 48 h, cells were washed in cold PBS and lysed at 4 °C in lysis buffer (10 mM Tris·HCl, pH 7.8/150 mM NaCl/1 mM EDTA/1% Nonidet P-40) containing protease inhibitor (Roche) and phosphatase inhibitor (Sigma). Equal amounts of protein lysates were incubated with mouse monoclonal anti-FLAG agarose conjugate at 4 °C.

Western Blotting. Western blotting was performed as described (14, 28). Primary antibodies included antibodies to anti-FLAG (Sigma; 1:5,000), anti-HA (Sigma; 1:2,000), anti-tubulin (Sigma; 1:2,000), anti-RRXS^{P} (Cell Signaling; 1:1,000), anti–PKC-α (Cell Signaling; 1:1,000), anti-WNK4 (28) (1:200), and anti-KLHL3 (Sigma; 1:1,000). Anti-WNK4 has been characterized using mice lacking *Wnk4* (28). Antibody against NCC was produced by immunizing rabbits with amino acids 76–97 of human NCC (74–95 of mouse and rat NCC). Specificity of the antibody was confirmed by comparing Western blots of kidney lysates from wild-type and NCC knockout mice (Fig. S3*D*). Characterization of anti-KLHL3 used in the study is shown in Fig. S5. The blot density was calculated digitally by using ImageJ.

AII Treatment. HEK cells were depleted of serum at least 12 h before experiment. After transient transfection of indicated plasmids, cells were stimulated with 100–250 nM AII. Inhibition of AT1R was performed with Losartan (1 μM), which was added 2 h before the addition of AII. Bisindolylmaleimide I and H89 were used at concentrations of 4 and 10 μM, respectively. These doses were used in previous cell-based studies to inhibit PKC and PKA activity (59, 60).

Immunofluorescence Microscopy. Cryosections from mouse kidneys were incubated with the indicated primary and secondary antibodies as described (14). To produce antibodies specific for KLHL3 phosphorylated at S433, the human KLHL3 peptide C-NTRRSS*VGVG (*phospho-Ser), conjugated to cysteine at the N terminus, was coupled to keyhole limpet hemocyanin, and rabbits were immunized with the phosphopeptides. Pooled serum was depleted of nonspecific antibodies with the cognate nonphosphopeptide, and the specific antibody was purified with the immunizing phosphopeptide. The antibody was used at a concentration of 1:600 for immunostaining.

In Vitro Kinase Assay. FLAG-tagged, full-length human KLHL3^{WT} and KLHL3^{S433N} were expressed in COS-7 cells seeded on 10-cm plates. After overnight serum starvation, cells were lysed with lysis buffer containing 1% Nonidet P-40, followed by incubation with mouse monoclonal anti-FLAG agarose conjugate at 4 °C. FLAG–KLHL3 was eluted by adding low-pH (pH 2.8) elution buffer (Thermo), followed by the addition of Tris (pH 9.0) for neutralization. A portion (5% of total by volume) of the purified KLHL3 was then incubated in the presence or absence of 0.3 U of PKC isozymes (PKC-α, PKC-β, and PKC-ε) in kinase buffer (20 mM Mops, pH 7.2, 25 mM β-glycerol phosphate, 1 mM sodium orthovanadate, 1 mM DTT, 1 mM $CaCl_2$, 12.5 mM $MgCl_2$, 80 μM ATP, 0.08 mg/mL phosphatidyl serine, and 6.25 μg/mL DAG) at 30 °C for 30 min. KLHL3 phosphorylation at S433 was analyzed by Western blotting using anti-RRXS^{P}. Signal specificity was confirmed by comparing the signal of KLHL3^{WT} with KLHL3^{S433N}. Purified, full-length PKC isozymes were obtained from Millipore.

Animal Studies. C57/B6 mice were maintained following a protocol approved by the Yale Institutional Animal Care and Use Committee (protocol no. 2008-10018). They were fed ad libitum and housed under a 12-h light cycle. Dietary manipulation included 8% (wt/wt) NaCl diet. AII was s.c. infused at a dose of 1 μg/kg per min for 48 h (14). Intensity of immunofluorescent staining of kidney sections for KLHL3$^{S433\text{-}P}$ from mice on a high-salt diet with or without AII infusion was evaluated by an observer

blinded to treatment status; samples identified as showing increased staining were all those treated with AII.

Statistical Analysis. The data are summarized as means ± SEM. Unpaired *t* test was used for comparisons between two groups. For multiple comparisons, statistical analysis was performed by ANOVA with Tukey's post hoc tests. P values < 0.05 were considered significant.

ACKNOWLEDGMENTS. We thank Toshiro Fujita for helpful discussions; Mary LoPresti and Jean Kanyo for assisting with protein digestion and MS data collections, respectively; and Hiromi Yamaguchi and Miyuki Fukazawa for help in immunofluorescence study and animal experiments. This work was supported in part by National Institutes of Health Grants P01-DK017433, P30-DK079310, UL1-RR024139, and P30-DA018343; and in part by Core Research for Evolutional Science and Technology (CREST) from Japan Science and Technology. R.P.L. is an investigator of the Howard Hughes Medical Institute.

1. Lifton RP, Gharavi AG, Geller DS (2001) Molecular mechanisms of human hypertension. *Cell* 104(4):545–556.
2. Wilson FH, et al. (2001) Human hypertension caused by mutations in WNK kinases. *Science* 293(5532):1107–1112.
3. Choi M, et al. (2011) K+ channel mutations in adrenal aldosterone-producing adenomas and hereditary hypertension. *Science* 331(6018):768–772.
4. Boyden LM, et al. (2012) Mutations in kelch-like 3 and cullin 3 cause hypertension and electrolyte abnormalities. *Nature* 482(7383):98–102.
5. Sacks FM, et al.; DASH-Sodium Collaborative Research Group (2001) Effects on blood pressure of reduced dietary sodium and the Dietary Approaches to Stop Hypertension (DASH) diet. *N Engl J Med* 344(1):3–10.
6. Mente A, et al.; PURE Investigators (2014) Association of urinary sodium and potassium excretion with blood pressure. *N Engl J Med* 371(7):601–611.
7. Kahle KT, Ring AM, Lifton RP (2008) Molecular physiology of the WNK kinases. *Annu Rev Physiol* 70:329–355.
8. Spät A, Hunyady L (2004) Control of aldosterone secretion: A model for convergence in cellular signaling pathways. *Physiol Rev* 84(2):489–539.
9. Abdallah JG, et al. (2001) Loop diuretic infusion increases thiazide-sensitive Na(+)/Cl(-)-cotransporter abundance: Role of aldosterone. *J Am Soc Nephrol* 12(7):1335–1341.
10. Pearce D, Kleyman TR (2007) Salt, sodium channels, and SGK1. *J Clin Invest* 117(3):592–595.
11. Beauwens R, Beaujean V, Zizi M, Rentmeesters M, Crabbé J (1986) Increased chloride permeability of amphibian epithelia treated with aldosterone. *Pflugers Arch* 407(6):620–624.
12. Fodstad H, et al. (2009) Effects of mineralocorticoid and K+ concentration on K+ secretion and ROMK channel expression in a mouse cortical collecting duct cell line. *Am J Physiol Renal Physiol* 296(5):F966–F975.
13. Welling PA (2013) Regulation of renal potassium secretion: Molecular mechanisms. *Semin Nephrol* 33(3):215–228.
14. Shibata S, et al. (2013) Mineralocorticoid receptor phosphorylation regulates ligand binding and renal response to volume depletion and hyperkalemia. *Cell Metab* 18(5):660–671.
15. Soleimani M, et al. (2012) Double knockout of pendrin and Na-Cl cotransporter (NCC) causes severe salt wasting, volume depletion, and renal failure. *Proc Natl Acad Sci USA* 109(33):13368–13373.
16. Kahle KT, et al. (2003) WNK4 regulates the balance between renal NaCl reabsorption and K+ secretion. *Nat Genet* 35(4):372–376.
17. Wilson FH, et al. (2003) Molecular pathogenesis of inherited hypertension with hyperkalemia: The Na-Cl cotransporter is inhibited by wild-type but not mutant WNK4. *Proc Natl Acad Sci USA* 100(2):680–684.
18. Yang CL, Angell J, Mitchell R, Ellison DH (2003) WNK kinases regulate thiazide-sensitive Na-Cl cotransport. *J Clin Invest* 111(7):1039–1045.
19. Kahle KT, et al. (2004) Paracellular Cl- permeability is regulated by WNK4 kinase: Insight into normal physiology and hypertension. *Proc Natl Acad Sci USA* 101(41):14877–14882.
20. Lalioti MD, et al. (2006) Wnk4 controls blood pressure and potassium homeostasis via regulation of mass and activity of the distal convoluted tubule. *Nat Genet* 38(10):1124–1132.
21. Ring AM, et al. (2007) An SGK1 site in WNK4 regulates Na+ channel and K+ channel activity and has implications for aldosterone signaling and K+ homeostasis. *Proc Natl Acad Sci USA* 104(10):4025–4029.
22. Ohta A, et al. (2013) The CUL3-KLHL3 E3 ligase complex mutated in Gordon's hypertension syndrome interacts with and ubiquitylates WNK isoforms: Disease-causing mutations in KLHL3 and WNK4 disrupt interaction. *Biochem J* 451(1):111–122.
23. Shibata S, Zhang J, Puthumana J, Stone KL, Lifton RP (2013) Kelch-like 3 and Cullin 3 regulate electrolyte homeostasis via ubiquitination and degradation of WNK4. *Proc Natl Acad Sci USA* 110(19):7838–7843.
24. Wakabayashi M, et al. (2013) Impaired KLHL3-mediated ubiquitination of WNK4 causes human hypertension. *Cell Reports* 3(3):858–868.
25. Lo SC, Li X, Henzl MT, Beamer LJ, Hannink M (2006) Structure of the Keap1:Nrf2 interface provides mechanistic insight into Nrf2 signaling. *EMBO J* 25(15):3605–3617.
26. Louis-Dit-Picard H, et al. (2012) KLHL3 mutations cause familial hyperkalemic hypertension by impairing ion transport in the distal nephron. *Nat Genet* 44(4):456–460, S451-453.
27. San-Cristobal P, et al. (2009) Angiotensin II signaling increases activity of the renal Na-Cl cotransporter through a WNK4-SPAK-dependent pathway. *Proc Natl Acad Sci USA* 106(11):4384–4389.
28. Castañeda-Bueno M, et al. (2012) Activation of the renal Na+:Cl- cotransporter by angiotensin II is a WNK4-dependent process. *Proc Natl Acad Sci USA* 109(20):7929–7934.
29. Herrera M, Coffman TM (2013) Control of electrolyte balance through ubiquitination. *Proc Natl Acad Sci USA* 110(19):7535–7536.
30. de Gasparo M, Catt KJ, Inagami T, Wright JW, Unger T (2000) International union of pharmacology. XXIII. The angiotensin II receptors. *Pharmacol Rev* 52(3):415–472.
31. Miller ML, et al. (2008) Linear motif atlas for phosphorylation-dependent signaling. *Sci Signal* 1(35):ra2.
32. Hein L, Meinel L, Pratt RE, Dzau VJ, Kobilka BK (1997) Intracellular trafficking of angiotensin II and its AT1 and AT2 receptors: Evidence for selective sorting of receptor and ligand. *Mol Endocrinol* 11(9):1266–1277.
33. Karim Z, Defontaine N, Paillard M, Poggioli J (1995) Protein kinase C isoforms in rat kidney proximal tubule: Acute effect of angiotensin II. *Am J Physiol* 269(1 Pt 1):C134–C140.
34. Natarajan R, Lanting L, Xu L, Nadler J (1994) Role of specific isoforms of protein kinase C in angiotensin II and lipoxygenase action in rat adrenal glomerulosa cells. *Mol Cell Endocrinol* 101(1-2):59–66.
35. Haller H, Quass P, Lindschau C, Luft FC, Distler A (1994) Platelet-derived growth factor and angiotensin II induce different spatial distribution of protein kinase C-alpha and -beta in vascular smooth muscle cells. *Hypertension* 23(6 Pt 2):848–852.
36. Adomeit A, et al. (1999) Bradykinin B(2) receptor-mediated mitogen-activated protein kinase activation in COS-7 cells requires dual signaling via both protein kinase C pathway and epidermal growth factor receptor transactivation. *Mol Cell Biol* 19(8):5289–5297.
37. Martel J, Dupuis G, Deschênes P, Payet MD (1998) The sensitivity of the human Kv1.3 (hKv1.3) lymphocyte K+ channel to regulation by PKA and PKC is partially lost in HEK 293 host cells. *J Membr Biol* 161(2):183–196.
38. O'Reilly M, et al. (2006) Dietary electrolyte-driven responses in the renal WNK kinase pathway in vivo. *J Am Soc Nephrol* 17(9):2402–2413.
39. Timmermans PB, et al. (1993) Angiotensin II receptors and angiotensin II receptor antagonists. *Pharmacol Rev* 45(2):205–251.
40. Mujais SK, Kauffman S, Katz AI (1986) Angiotensin II binding sites in individual segments of the rat nephron. *J Clin Invest* 77(1):315–318.
41. Gurley SB, et al. (2011) AT1A angiotensin receptors in the renal proximal tubule regulate blood pressure. *Cell Metab* 13(4):469–475.
42. van der Lubbe N, et al. (2011) Angiotensin II induces phosphorylation of the thiazide-sensitive sodium chloride cotransporter independent of aldosterone. *Kidney Int* 79(1):66–76.
43. Mamenko M, Zaika O, Ilatovskaya DV, Staruschenko A, Pochynyuk O (2012) Angiotensin II increases activity of the epithelial Na+ channel (ENaC) in distal nephron additively to aldosterone. *J Biol Chem* 287(1):660–671.
44. Gonzalez-Villalobos RA, et al. (2013) The absence of intrarenal ACE protects against hypertension. *J Clin Invest* 123(5):2011–2023.
45. Wei Y, Zavilowitz B, Satlin LM, Wang WH (2007) Angiotensin II inhibits the ROMK-like small conductance K channel in renal cortical collecting duct during dietary potassium restriction. *J Biol Chem* 282(9):6455–6462.
46. Crowley SD, et al. (2005) Distinct roles for the kidney and systemic tissues in blood pressure regulation by the renin-angiotensin system. *J Clin Invest* 115(4):1092–1099.
47. Bhalla V, et al. (2005) Serum- and glucocorticoid-regulated kinase 1 regulates ubiquitin ligase neural precursor cell-expressed, developmentally down-regulated protein 4-2 by inducing interaction with 14-3-3. *Mol Endocrinol* 19(12):3073–3084.
48. Gao M, et al. (2004) Jun turnover is controlled through JNK-dependent phosphorylation of the E3 ligase Itch. *Science* 306(5694):271–275.
49. Takahashi D, et al. (2013) KLHL2 interacts with and ubiquitinates WNK kinases. *Biochem Biophys Res Commun* 437(3):457–462.
50. Soltysik-Espanola M, et al. (1999) Characterization of Mayven, a novel actin-binding protein predominantly expressed in brain. *Mol Biol Cell* 10(7):2361–2375.
51. Rinehart J, et al. (2009) Sites of regulated phosphorylation that control K-Cl cotransporter activity. *Cell* 138(3):525–536.
52. Chen L, Gilkes DM, Pan Y, Lane WS, Chen J (2005) ATM and Chk2-dependent phosphorylation of MDMX contribute to p53 activation after DNA damage. *EMBO J* 24(19):3411–3422.
53. Winter M, et al. (2008) Control of HIPK2 stability by ubiquitin ligase Siah-1 and checkpoint kinases ATM and ATR. *Nat Cell Biol* 10(7):812–824.
54. Santra MK, Wajapeyee N, Green MR (2009) F-box protein FBXO31 mediates cyclin D1 degradation to induce G1 arrest after DNA damage. *Nature* 459(7247):722–725.
55. Santini S, et al. (2013) ATM kinase activity modulates ITCH E3-ubiquitin ligase activity. *Oncogene* 33(9):1113–23.
56. Mu S, et al. (2011) Epigenetic modulation of the renal β-adrenergic-WNK4 pathway in salt-sensitive hypertension. *Nat Med* 17(5):573–580.
57. Hebert SC, Culpepper RM, Andreoli TE (1981) NaCl transport in mouse medullary thick ascending limbs. II. ADH enhancement of transcellular NaCl cotransport; origin of transepithelial voltage. *Am J Physiol* 241(4):F432–F442.
58. Haque MZ, Caceres PS, Ortiz PA (2012) β-Adrenergic receptor stimulation increases surface NKCC2 expression in rat thick ascending limbs in a process inhibited by phosphodiesterase 4. *Am J Physiol Renal Physiol* 303(9):F1307–F1314.
59. Harada H, et al. (1999) Phosphorylation and inactivation of BAD by mitochondria-anchored protein kinase A. *Mol Cell* 3(4):413–422.
60. Walker AJ, Plows LD (2003) Bacterial lipopolysaccharide modulates protein kinase C signalling in Lymnaea stagnalis haemocytes. *Biol Cell* 95(8):527–533.